24th INTERNATIONAL CONGRESS ON SOUND AND VIBRATION
23–27 July 2017, London

STUDY ON THE PRODUCIBILITY OF ADDITIVELY MANUFACTURED ACOUSTIC BLACK HOLES

Sebastian Rothe, Hagen Watschke and Sabine C. Langer
TU Braunschweig – Institut für Konstruktionstechnik, 38106 Braunschweig, Germany
email: sebastian.rothe@tu-braunschweig.de

Acoustic black holes are a smart passive method to focus structure-borne sound in thin components. By decreasing the mechanical impedance of the structure through a thickness diminution based on a certain form function, the bending waves are directed towards a specific location. By means of a damping application in this area, the whole component can be damped efficiently. To produce such a set-up, the structure has to be edited by a post-processing, e.g. with the help of milling cutters. Subsequently, an additional damping measure, for example to realize constrained-layer damping, has to be applied. However, this is time consuming and leads to increasing costs and a change in the external geometry of the overall construction.

Additive manufacturing offers new design potentials in relation to the required properties which should be taken into account beforehand, such as the consideration of specific impedance adjustments within the structure. Furthermore, additional damping can be introduced into the system with the help of various material combinations. The new design freedom facilitates the shaping of the outer topology, independent of the acoustic black hole.

In this work, beam structures with different shapes of acoustic black holes are investigated and compared with a simple reference beam. The additively manufactured samples are experimentally tested and compared with numerical calculations. The various possibilities of additive manufacturing result in a larger variety of acoustic black hole designs than with conventional manufacturing processes. The benefits and the effectiveness of using additive manufacturing to apply these innovative passive damping measures are discussed.

Keywords: acoustic black holes, additive manufacturing, vibroacoustic, finite element method

1. Introduction

A major challenge in product design is to develop lightweight as well as low noise structures. It results in the basic conflict of an increasing sound radiation of the components with increasing relative stiffness of the materials. To resolve this conflict, the method of Acoustic Black Holes (ABH) promises a great possibility [1]. However, this damping method results in an increased complexity in manufacturing and assembling caused by the special ABH shapes as well as the integration of additional damping by application of different materials into the structure.

Based on the layer-wise material deposition working principle of additive manufacturing (AM) processes, a new design freedom is enabled in contrast to traditional manufacturing processes for ABH. Milling is the most frequently used manufacturing method to produce parts with ABH by cutting shapes of the holes and applying additional damping layers on the components. *Boyer et al.* [2] show that milling is not the solution to promote ABH for industrial applications. They suggest AM as a promising possibility. Specifically, AM enables the manufacturability of virtually any shape without additional costs and facilitates the combination of different materials in one process without any joining operation [3]. Due to the integration of flexible materials with specific shapes, AM offers a high potential for the integration of acoustic functions, ABH in particular.

The main objective of this paper is to show the feasibility of additively manufactured ABH. Therefor, experimental investigations on simple beam structures with different ABH shapes are done and compared with numerical calculations. In addition, advantages of the new manufacturing freedom are discussed.

1.1 Method of Acoustic Black Holes

The method of ABH is a smart passive measure for noise reduction, in which a specific attenuation is introduced into thin structures. Due to a smooth thickness reduction in a local area, the flexural waves propagate in the direction of the ABH, decelerate and their amplitudes increase along the material diminution. The reason is the decrease of the mechanical impedance. This effect was first described by *Mironov* [4]. The result is an area for an efficient damping placement, e.g. an application of additional damping material in the ABH. The name *Acoustic Black Hole* was first introduced by *Krylov*, who investigated the effect on plate edges in 2000 [5].

To generate the ABH effect, the thickness reduction has to follow a special power law. *Mironov* proposes the following shape function s [4]:

$$s(x) = ax^n + b \qquad with \qquad a = \frac{h_{max} - h_{min}}{l_{ABH}^n}, \quad b = h_{min}, \quad n \geq 2. \tag{1}$$

The geometric variables h_{max} and h_{min} describe the maximal and the minimal height, l_{ABH} the length of the ABH. The n represents the power coefficient of the shape function and should be greater or equal 2. A sketch of an ABH shape function is shown in Fig. 1. As power coefficient, $n = 10$ is chosen. This applies to all further investigations in this paper, too.

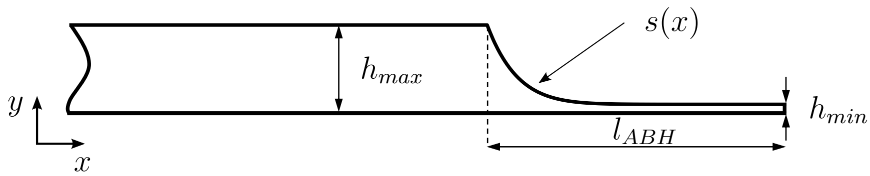

Figure 1: Sketch of an exemplary ABH shape function ($n = 10$).

Preliminary investigations already show the importance of position [6] as well as the type of shape function [7] of the ABH regarding the efficiency in noise reduction. This effect could be used even better with the manufacturing freedom of AM.

1.2 Additive Manufacturing

Additive manufacturing has progressed from solely a rapid prototyping technology to a process for facilitation of end-use products. Especially the processes of Selective Laser Melting (SLM), Selective Laser Sintering (SLS) and Fused Deposition Modeling (FDM) have been utilized for production applications [8]. The new design possibilities enabled by these AM technologies can generally be categorized into shape complexity, hierarchical complexity, functional complexity and material complexity [3]. On the one hand, shape complexity and hierarchical complexity offer, for example, the realization of customized shapes and the utilization of internal graded lattice structures. On the other hand, functional complexity describes the design potential to embed additional components during the manufacturing process, e.g. sensors, or to manufacture fully functional components like ball bearings without necessary assembly operations. The layer-by-layer process further allows the integration of multiple materials into one part. Even though the different AM processes provide, in general, the same design potentials, the degree of the design freedom is specific for the particular process.

To manufacture ABH by AM, a process is necessary integrating both hard and soft materials into one part. Thus, an impedance reduction by fully filled design space and a constrained-layer damping can be realized by combining two types of material. This potential is specific for the FDM technology. For this reason, it suits best for the manufacturing of ABH.

In Fig. 2, the FDM's principle is shown. Initially, the material is melted in a heating element and layer-wise deposited on the build platform. The build platform moves down in z direction and the next layer material is selectively deposited again. The two extrusion nozzles allow combining different materials regarding specific product requirements. In *Watschke et al.* [9], this has already been shown for the integration of conductive functions.

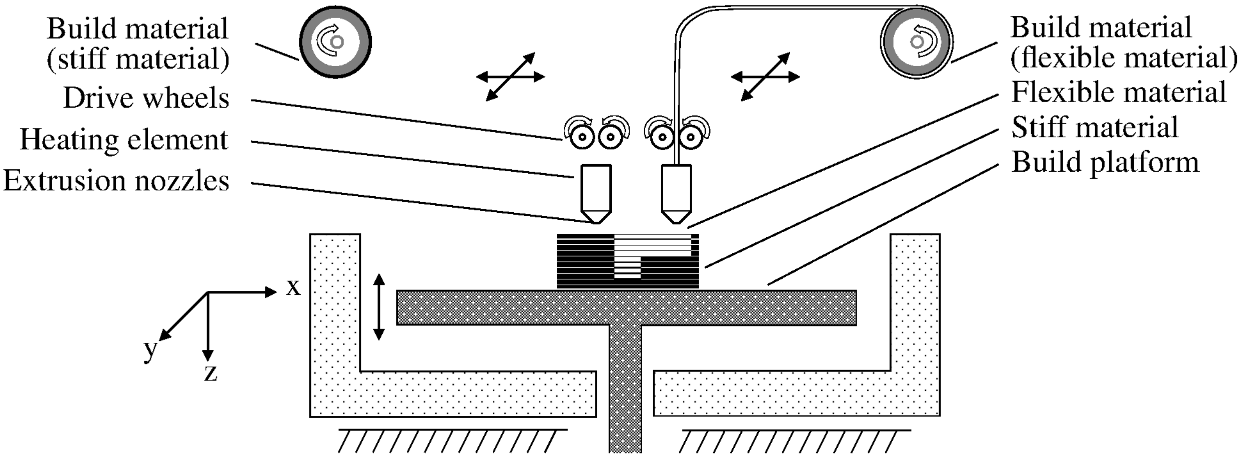

Figure 2: Principle of Fused Deposition Modeling process; adapted from [10].

2. Investigation setup

In this section, the setup and the work flow to manufacture ABH by AM and to characterize them acoustically are described. The following subsections present the main steps in detail. The basis of the investigation is a simple 0.260 x 0.020 x 0.006 m beam structure with three different areas: a clamped area for the experimental investigations, a non-design area and a design area, where the different ABH shapes are applied. A point force (red arrow in Fig. 3) excites the beam 0.03 m away from the border between non-design and clamped area. Details can be found in Fig. 3.

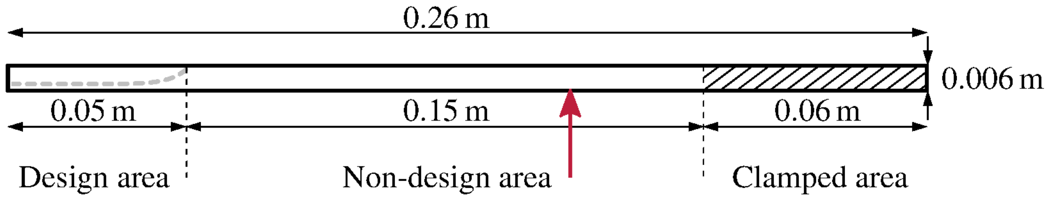

Figure 3: Sketch of the reference beam structure with (ABH) design, non-design and clamped area.

The reference beam structure is additively manufactured only with the base material. It is the reference for all investigations.

2.1 Determination of material properties

Since the process parameters of the additive manufacturing process mainly influence the resultant material properties, a preliminary investigation is required for the characterization of the utilized materials. Therefor, test specimens according to DIN EN 527 are manufactured beforehand and tested by tensile test to determine the tensile modulus specific to the selected process parameters. On the one hand, Polylactide (PLA) with a measured average tensile modulus of 3272.1 MPa is used for the rigid part. On the other hand, the flexible part and damping structure, respectively, is manufactured of a specially formulated thermoplastic polyurethane (TPU) material called NinjaFlex® [1]. The measured tensile modulus of the TPU is 11.5 MPa, and thus, about a factor of 285 smaller than the tensile modulus of PLA. Table 1 provides an overview of the determined material parameters.

Table 1: Material properties.

Description	Variable	Unit	PLA	TPU
E-modulus	E	[N/m^2]	3.2721E9	0.0115E9
Density	ϱ	[kg/m^3]	1226	1166
Poisson ratio	ν	[–]	0.35	0.35

In addition, the frequency dependent damping of the hybrid composite must be determined. For this, on the one hand, a 1 mm TPU layer is printed on the reference beam structure (*Damp Reference*) and, on the other hand, a sample with 3 mm TPU and 3 mm PLA (*Damp Reference 2*) is manufactured (see Figure 4). The damping of the clamped *Damp Reference* is approximately three times higher than the damping of the *Reference* beam.

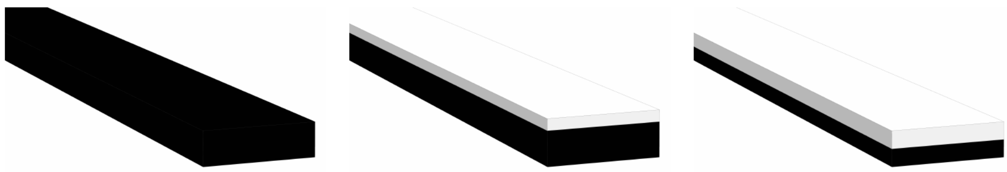

(a) *Reference* (6 mm PLA) (b) *Damp Reference* (6 mm PLA, 2 mm TPU) (c) *Damp Reference 2* (3 mm PLA, 3 mm TPU)

Figure 4: Investigated reference beams.

With the help of a decay test and the two samples with different layer heights, the loss factor can be calculated according to the approach of *Oberst* [11]. Based on these material characterizations, the determined values are utilized for the numerical calculations of the ABH.

2.2 Manufactured ABH

As already described in Section 1.1, a power law shape function with a power coefficient $n = 10$ is used for all ABH. In order to achieve as much damping as possible, the omitted PLA region is fully filled by TPU. Thus, the external geometry of the beams remains the same as the one of the *Reference*. All investigated beams with ABH are shown in Fig. 5.

For the first black hole (*ABH 1*), the PLA reduction is performed from one side, as with most ABH in literature. To shape the second ABH beam (*ABH 2*), the form function is applied from both sides,

[1]Flexible 3D printing filament of the company NinjaTek (USA)

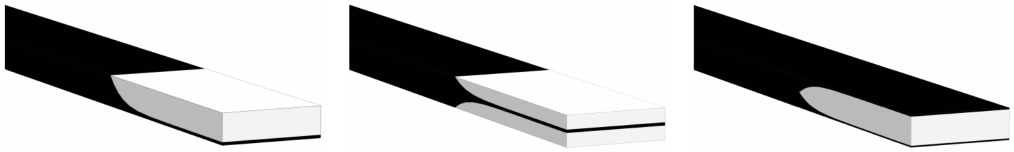

(a) *ABH 1* (b) *ABH 2* (c) *ABH 3*

Figure 5: Investigated ABH shapes.

starting from outside to the center of the beam. The third ABH beam (*ABH 3*) is the inversed case of *ABH 2*. The form function is applied two times, starting from the middle to the outside of the beam. It is an exemplary case which can only be realized with the help of the AM. There are two ABH that are integrated into the structure without changing the cover material on the bottom and the top. This could be an interesting application in industry, e.g. to protect the damping material chemically or/and mechanically.

2.3 Numerical preliminary studies

Before the beams are studied experimentally, the expected behavior is estimated numerically using the Finite-Element-Method. Therefor, the reference beams (*Reference*, *Damp Reference*) and the beams with black hole (*ABH 1*, *ABH 2*, *ABH 3*) are modeled by fully integrated hexahedron volume elements with quadratic shape functions. The element discretization is verified by means of a convergence study. At least five nodes across the beam thickness are selected. An exemplary mesh of *ABH 2* is shown in Fig. 6.

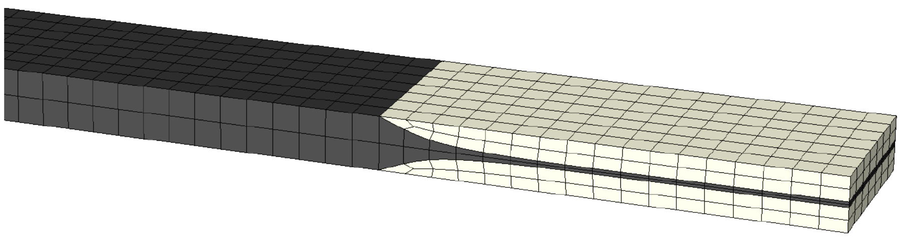

Figure 6: Volume mesh of *ABH 2*.

The geometric data and boundary conditions of the beam structures can be extracted from Fig. 3. A harmonic point force in a frequency range between 1 and 3500 Hz is modeled as dynamic excitation. The used materials are listed in Table 1. A linear isotropic material law is used. To simulate the frequency-dependent damping, the examined damping data (see Section 2.1) is fitted by a *Rayleigh*-damping curve. The found mass proportional parameter α and the stiffness proportional parameter β (see [12]) are defined in the Finite-Element-Model.

2.4 Experimental investigations

For the experimental measurement of the admittance of the additively manufactured structures, the beams are clamped between two steel bricks. An electro-dynamic shaker is used for excitation. The force is measured by means of a load cell. The investigated beam samples are shown in Fig. 7 (a), as well as the experimental setup (b) with the *ABH 2* beam sample.

To measure the resulting vibrations (surface velocity), a laser-scanning vibrometer is used. In order to guarantee a better reflecting surface, the samples are laminated with a reflection foil.

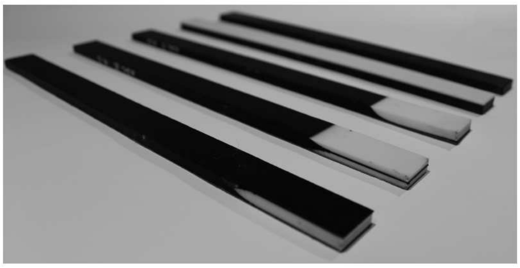

(a) Overview of investigated beam samples

(b) Clamped beam sample (*ABH 2*)

Figure 7: Beam samples and experimental setup.

3. Results and discussion

The frequency response function (FRF) of the mean square admittance is determined and compared. The expected behavior of the dynamic systems is, that the acoustic black hole effect becomes stronger in higher frequencies compared to lower frequencies. This follows due to the decreasing bending wave length in the structure with higher frequency. They are increasingly focussed in the ABH and can be efficiently damped by the combination with TPU. For a reasonably fair comparison, the results of the ABH beams are compared to the *Damp Reference*, where the applied TPU-layer leads to an additional damping. Nevertheless, the FRF of the *Reference* is shown as well.

The results of the preliminary numerical study can be observed in Fig. 8. It represents the scientific findings of an ideal and simple modeling of the described problem.

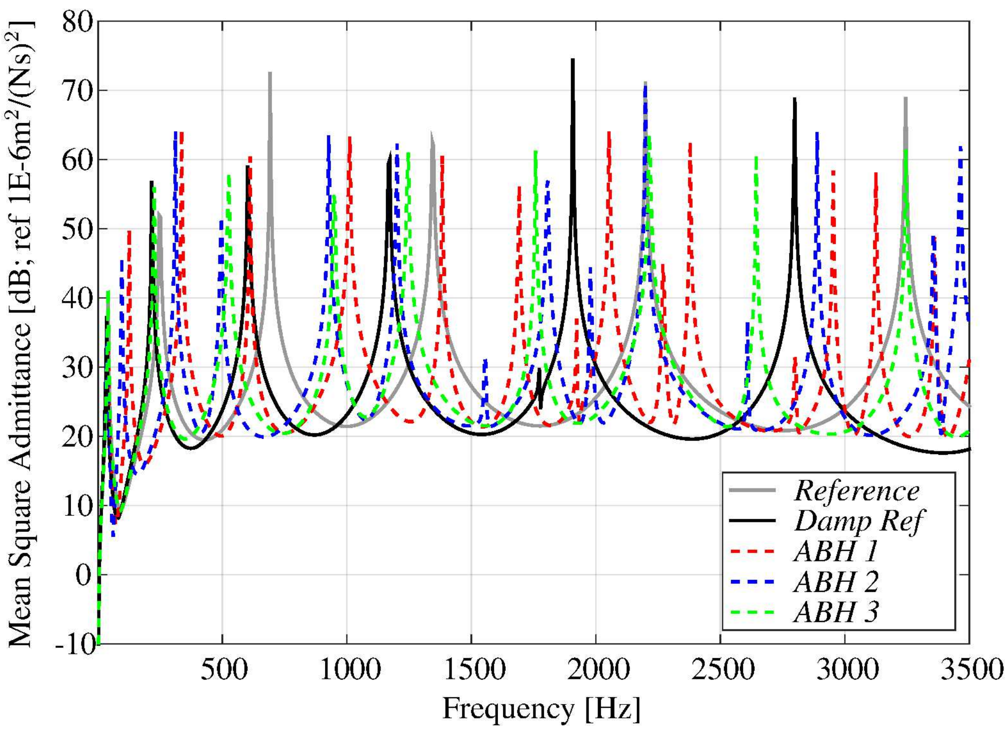

Figure 8: Results of numerical investigations.

For the beams with ABH an increase of the modal density can be seen. This effect appears due a less stiff beam structure because of the weakening by the ABH. The expected stronger ABH effect in higher frequencies can be observed. From 1500 Hz, the resonance peaks of the ABH beams are 5 to

10 dB lower than the peaks of the *Damp Reference* beam. Under 1500 Hz, there is no large difference. This pattern should be distinguishable at the experimental results, too. Within the FRF of *ABH 1*, the largest ABH effect can be recognized, followed by *ABH 3* and *ABH 2*.

In Fig. 9, the experimentally determined mean square admittance of the different specimen is compared. The ABH effects are also visible in this plot. There is an increased damping of the peaks in higher frequencies at all ABH beams. *ABH 1* leads to the largest effect, as seen in Fig. 8. But especially *ABH 3*, which can only be manufactured with the freedom of AM, shows a good alternative to the "standard" *ABH 1* and has advantages in application because of the top and bottom cover made of basic material. The peak difference between all specimens' FRFs below 1500 Hz is small, too.

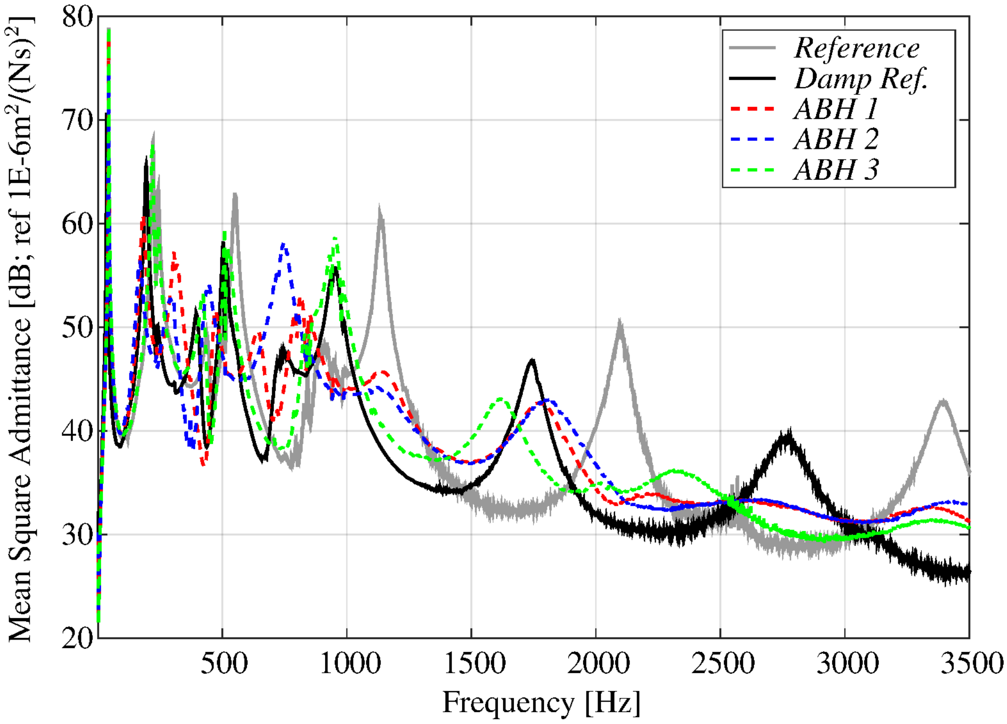

Figure 9: Comparision of experimental results.

Qualitatively, the effects of the numerical investigations can be shown in the experiment. Nevertheless, a quantitative comparison shows large differences in the dynamic behavior of the beams. The reasons for this can be different. The printed materials are simplified linearly isotropically modeled, although they have anisotropic material behavior. Moreover, the continuous descent of the FRF in Fig. 9 could be caused by uncertainties in the experiment. An ideal clamped boundary condition is numerically modeled but can not be realized in experiment. Furthermore, the vibration of the shaker and the test stand could influence the results in the lower frequencies because of their high mass, compared to the mass of the plastic beam, and a not ideal stiff behavior. In addition, errors may have occurred during the determination of the damping.

4. Conclusion and future outlook

The results of this work show that it is feasible to manufacture ABH by AM. The ABH effect could be shown numerically and experimentally. For this purpose, different black hole shapes were defined. By combination of the basic material PLA with the more flexible material TPU, an additional damping effect in the ABH was realized. Particularly the results of the integrated *ABH 3*, which can only be manufactured by AM, show the great potential of additively manufactured ABH. New features can be provided to the component, e.g. by an encapsulated ABH in the basic material. Thus, the damping material could be protected from external influences.

For future works, the experimental and numerical model setup have to be improved and validated. In addition, other manufacturing freedoms of AM should be tested, like internal lattice structures or other material combinations, to optimize the acoustic and lightweight characteristics.

REFERENCES

1. Krylov, V. V. Acoustic black holes: recent developments in the theory and applications, *IEEE Transactions on Ultrasonics, Ferroelectrics, and Frequency Control*, **61** (8), 1296–1306, (2014).

2. Bowyer, E. P., Krylov, V. V. Acoustic black hole manufacturing for practical applications and the effect of geometrical and material imperfections, *Proceedings of the inter.noise*, Hamburg, Germany, 21–24 August, (2016).

3. Gibson, I., Rosen, D., Stucker, B., *Additive Manufacturing Technologies: 3D Printing, Rapid Prototyping, and Direct Digital Manufacturing*, Springer, New York, (2015).

4. Mironov, M. A. Propagation of a flexural wave in a plate whose thickness decreases smoothly to zero in a finite interval, *Soviet Physics Acoustics-USSR*, **34** (3), 318–319 (1988).

5. Krylov, V. V. and Shuvalov, A. L. Propagation of localised flexural vibrations along plate edges described by a power law, *Proceedings of the Institute of Acoustics*, **22**, 263–270, (2000).

6. Rothe, S., Ghaffari Mejlej, V., Langer, S. C. and Vietor, T. Optimal adaptation of acoustic black holes by evolutionary optimization algorithms, PAMM, **16** (1), 625–626, (2016).

7. Rothe, S., Dorn, M. and Langer, S. C. Numerical study on shape functions for optimal exploitation of the acoustic black hole effect, PAMM, not yet published, (2017).

8. VDI-Fachbereich Produktionstechnik und Fertigungsverfahren, *Additive Fertigungsverfahren - Grundlagen, Begriffe, Verfahrensbeschreibungen*, standard VDI 3405, VDI-Gesellschaft Produktion und Logistik, (2014).

9. Watschke, H., Rautenberg, D., Waalkes, L., Junior, C. and Vietor, T. Integration of conductive functions based on Fused Layer Modeling, *Proceedings of the 14th Rapid.Tech Conference*, Erfurt, Germany, 20–22 June, (2017).

10. Ottnand, T., *Dosierung von Kunststoffen für generative Fertigungsverfahren*, PhD Thesis, Technical University of Munich, (2014).

11. Oberst, H. and Frankenfeld, K. Über die Dämpfung der Biegeschwingungen dünner Bleche durch fest haftende Beläge, *Acta Acustica united with Acustica*, **2** (6), 181–194, (1952).

12. Nasdala, L. *FEM-Formelsammlung Statik und Dynamik: Hintergrundinformationen, Tipps und Tricks*, Springer, New York, (2015).